Majorana edge states in superconductor-noncollinear magnet interfaces

Wei Chen[1,2] and Andreas P. Schnyder[2]
[1]*Theoretische Physik, ETH-Zürich, CH-8093 Zürich, Switzerland*
[2]*Max-Planck-Institut für Festkörperforschung, Heisenbergstrasse 1, D-70569 Stuttgart, Germany*
(Received 9 April 2015; revised manuscript received 16 November 2015; published 4 December 2015)

Through $s-d$ coupling, a superconducting thin film interfaced to a noncollinear magnetic insulator inherits its magnetic order, which may induce unconventional superconductivity that hosts Majorana edge states. We present a unified formalism that covers the cycloidal, helical, and tilted conical order discovered in multiferroics, as well as Bloch and Neel domain walls of ferromagnetic insulators, and show that they induce (p_x+p_y)-wave pairing that supports Majorana edge modes. The advantages over one-dimensional proposals are that the Majorana states can exist without fine tuning of the chemical potential, can be stabilized in a much larger parameter space, and can be separated over the distance of long-range noncollinear order that is known to reach a macroscopic scale. A skyrmion spin texture, on the other hand, induces a nonuniform (p_r+ip_φ)-wave-like pairing under the influence of an emergent electromagnetic field, yielding a vortex state that displays both a bulk persistent current and a topological edge current.

DOI: 10.1103/PhysRevB.92.214502 PACS number(s): 73.20.−r, 71.10.Pm, 73.21.−b, 74.45.+c

I. INTRODUCTION

Motivated by possible applications in non-Abelian quantum computation [1], the search for Majorana fermions in condensed-matter systems has witnessed a boost recently [2–6]. Indeed there has been much effort to design and fabricate one-dimensional heterostructures in which topological p-wave superconductivity is proximity induced [7–13]. One particularly promising proposal is chains of magnetic atoms with noncollinear spin texture on the surface of a conventional superconductor (SC) [14–24]. The presence of these magnetic adatoms induces Shiba bound states [25–27], whose low-energy physics is equivalent to a one-dimensional (1D) p-wave SC with Majorana modes at its ends. Scanning tunneling measurements of zero-bias peaks at the ends of Fe chains deposited on superconducting Pb have been interpreted as evidence of Majorana modes [28], although no general consensus has been reached regarding the definitive existence of Majorana states in these systems [29].

Since thin films are generally easier to manufacture than adatoms, it is intriguing to ask if such 1D proposals can be generalized to two-dimensional (2D) systems, where a superconducting thin film is coupled to a noncollinear magnet. The work by Nakosai *et al.* [30] first shed light on this issue. It was found that a spiral spin texture in proximity to an s-wave SC induces a (p_x+p_y)-wave state that exhibits bulk nodes and Majorana flat-band edge states, while a skyrmion crystal spin configuration induces a full gap with chirally dispersing Majorana edge states that is interpreted as a result of (p_x+ip_y)-wave-like pairing. In this paper, we show that these phenomena occur in a much broader class of superconductor-noncollinear magnet interfaces. In particular, we find that a great variety of noncollinear magnets, including multiferroic insulators with helical, cycloidal, and (tilted) conical order, as well as magnetic domain walls of ferromagnetic (FM) insulators, interfaced with an s-wave SC induce a (p_x+p_y)-wave pairing state with Majorana flat bands at the boundary. We derive a general criterion for the appearance of Majorana edge states that applies to all of the aforementioned superconductor-noncollinear magnet interfaces. It is shown that the Majorana modes occur without fine tuning of the chemical potential, and that Majorana pairs can be separated over macroscopic distances. Furthermore, we investigate a single skyrmion spin texture coupled to an s-wave SC and rigorously derive an induced inhomogeneous (p_r+ip_φ)-wave-like pairing, which coexists with the emerging electromagnetic field induced by the noncoplanar spin texture.

II. SC/MULTIFERROIC INTERFACE

Evidence from the T_c reduction in magnetic oxide/SC heterostructures [31,32] suggests that an $s-d$ coupling, $\Gamma\mathbf{S}_i\cdot\boldsymbol{\sigma}$, generally exists at the interface atomic layer between an SC and an insulating magnetic oxide [33], where $\boldsymbol{\sigma}$ is the conduction electron spin and $\mathbf{S}_i$ is the local moment. This leads us to consider the following model for the SC/multiferroic interface, which is the 2D generalization of the 1D proposals of Refs. [14,15]:

$$H=\sum_{i,\delta,\alpha}\left(t_{i\delta}f^\dagger_{i\alpha}f_{i+\delta\alpha}+t^*_{i\delta}f^\dagger_{i+\delta\alpha}f_{i\alpha}\right)-\mu\sum_{i,\alpha}f^\dagger_{i\alpha}f_{i\alpha}+\sum_{i,\alpha,\beta}(\mathbf{B}_i\cdot\boldsymbol{\sigma})_{\alpha\beta}f^\dagger_{i\alpha}f_{i\beta}+\sum_i\Delta_0\left(f^\dagger_{i\uparrow}f^\dagger_{i\downarrow}+f_{i\downarrow}f_{i\uparrow}\right),\tag{1}$$

where $i=\{i_x,i_y\}$ is the site index, $\hat{\boldsymbol{\delta}}=\{\hat{\mathbf{a}},\hat{\mathbf{b}}\}$ is the planar unit vector, and α is the spin index. In the absence of spin-orbit interaction, the majority of the noncollinear order discovered in multiferroics, for instance in perovskite rare-earth manganites [34–37], can be generically described by the conical order,

$$\mathbf{B}_i=\left(B_i^x,B_i^y,B_i^z\right)=(B_\parallel\sin\theta_i,B_\perp,B_\parallel\cos\theta_i),\tag{2}$$

as far as their effect on the SC is concerned, since the choice of coordinate for $\boldsymbol{\sigma}$ is arbitrary. For instance, cycloidal and helical order are equivalent by trivially exchanging two components of $\boldsymbol{\sigma}$. Tilted conical orders with any tilting angle are equivalent to untitled conical orders. In Eq. (2), $B_\parallel=\Gamma|\mathbf{S}_{i\parallel}|$ and $B_\perp=\Gamma|\mathbf{S}_{i\perp}|$ are the planar and out-of-plane components of

the local moment, respectively. The planar angle $\theta_i = \mathbf{Q}\cdot\mathbf{r}_i$ is determined by the spiral wave vector $\mathbf{Q}$ and the planar position $\mathbf{r}_i$. Cycloidal order corresponds to the case where $B_\perp\hat{\mathbf{y}} = 0$. Note that a three-dimensional conical order projected to a surface cleaved at any direction is also described by Eq. (2). So, our formalism is applicable to a thin film or the surface of a single-crystal multiferroic in any crystalline orientation, assuming no lattice mismatch with the SC and a constant $|\mathbf{S}_i| = |\mathbf{S}|$, which, in principle, can also take into account quantum or thermal fluctuations.

The third term in Eq. (1) can be brought into diagonal form in spin space by performing two consecutive rotations to align the $\mathbf{B}_i$ field along σ^z,

$$\begin{pmatrix} f_{i\uparrow} \\ f_{i\downarrow} \end{pmatrix} = \begin{pmatrix} \cos\frac{\theta_i}{2} & -\sin\frac{\theta_i}{2} \\ \sin\frac{\theta_i}{2} & \cos\frac{\theta_i}{2} \end{pmatrix} \begin{pmatrix} \cos\frac{\gamma}{2} & i\sin\frac{\gamma}{2} \\ i\sin\frac{\gamma}{2} & \cos\frac{\gamma}{2} \end{pmatrix} \begin{pmatrix} g_{i\uparrow} \\ g_{i\downarrow} \end{pmatrix} = U_i \begin{pmatrix} g_{i\uparrow} \\ g_{i\downarrow} \end{pmatrix}, \tag{3}$$

where $\sin\gamma = B_\perp/B_0$ and $B_0 = \sqrt{B_\parallel^2 + B_\perp^2} = |\Gamma\mathbf{S}|$. This yields

$$\begin{aligned} H = &\sum_{i,\delta,\alpha,\beta} \left(t_{i\delta}\Omega_{i\delta\alpha\beta} g^\dagger_{i\alpha} g_{i+\delta\beta} + t^*_{i\delta}(\Omega^*_{i\delta})_{\beta\alpha} g^\dagger_{i+\delta\alpha} g_{i\beta}\right) \\ &+ \sum_{i,\alpha,\beta} \left(B\sigma^z_{\alpha\beta} - \mu I_{\alpha\beta}\right) g^\dagger_{i\alpha} g_{i\beta} \\ &+ \sum_i \Delta_0 \left(g^\dagger_{i\uparrow} g^\dagger_{i\downarrow} + g_{i\downarrow} g_{i\uparrow}\right), \end{aligned} \tag{4}$$

$$\Omega_{i\delta} = U_i^\dagger U_{i+\delta} = \begin{pmatrix} \alpha_{i\delta} & -\beta^*_{i\delta} \\ \beta_{i\delta} & \alpha^*_{i\delta} \end{pmatrix},$$

$$\alpha_{i\delta} \equiv \alpha_\delta = \cos\frac{\mathbf{Q}\cdot\boldsymbol{\delta}}{2} - i\sin\gamma\sin\frac{\mathbf{Q}\cdot\boldsymbol{\delta}}{2},$$

$$\beta_{i\delta} \equiv \beta_\delta = \cos\gamma\sin\frac{\mathbf{Q}\cdot\boldsymbol{\delta}}{2}.$$

In what follows, we consider hopping to be real and isotropic, $t_{i\delta} = t^*_{i\delta} = t$.

In the limit $B_0 \approx |\mu| \gg \{t, \Delta_0\}$ with $\mu < 0$, one can construct an effective low-energy theory for the spin species near the Fermi level, which is the spin-down band. This is done by introducing a unitary transformation $H' = e^{-iS} H e^{iS}$ to eliminate the spin mixing terms order by order [14]. At first order, the pairing part,

$$H_{\text{eff},\Delta} = \sum_{i,\delta} \left[\left(\frac{1}{B} - \frac{1}{\mu}\right)\Delta_0 t \beta^*_{i\delta} g_{i\downarrow} g_{i+\delta\downarrow} + \text{H.c.}\right], \tag{5}$$

resembles a spinless p-wave SC with anisotropic nearest-neighbor and next-nearest-neighbor hopping. From Eq. (4), one has $\beta^*_{i\delta} = \cos\gamma\sin\mathbf{Q}\cdot\boldsymbol{\delta}/2$, so the induced pairing is of $(p_x + p_y)$-wave symmetry, with the magnitude of the gap determined by the wavelength of the planar component of the conical order.

To derive the criterion for the appearance of Majorana edge states, we introduce Majorana operators $g_{i\sigma} = \frac{1}{2}(b_{i1\sigma} + ib_{i2\sigma})$, $g^\dagger_{i\sigma} = \frac{1}{2}(b_{i1\sigma} - ib_{i2\sigma})$ with $\{b_{im\alpha}, b_{i'm'\beta}\} = 2\delta_{ii'}\delta_{mm'}\delta_{\alpha\beta}$, and express the Hamiltonian $H = (i/4)\sum_{\mathbf{q}} b^\dagger_{\mathbf{q}} A(\mathbf{q}) \mathbf{b}_{-\mathbf{q}}$ in terms of the basis $b^\dagger_{\mathbf{q}} = (b_{\mathbf{q}1\uparrow}, b_{\mathbf{q}1\downarrow}, b_{\mathbf{q}2\uparrow}, b_{\mathbf{q}2\downarrow})$ [15]. We choose open boundary conditions (OBCs) along $\hat{\mathbf{x}}$ and periodic ones (PBCs) along $\hat{\mathbf{y}}$, such that $-\pi < q_y < \pi$ is a good quantum number. For a given q_y, the Majorana Hamiltonian $A(q_x, q_y)$ is skew symmetric only when q_x satisfies

$$\beta_a \sin q_x + \beta_b \sin q_y = 0. \tag{6}$$

The two solutions q_{x1} and q_{x2} of Eq. (6) are high symmetry points at which the Pfaffian of the Majorana Hamiltonian is well defined. Hence, we can introduce the following topological index [15]:

$$M(q_y) = \text{Sign}\{\text{Pf}[A(q_{x1}, q_y)]\}\text{Sign}\{\text{Pf}[A(q_{x2}, q_y)]\}, \tag{7}$$

which depends on the edge momentum q_y. $M(q_y) = -1$ signals a topologically nontrivial character with Majorana edge states at q_y. That is, the condition for the existence of Majorana states reads

$$\begin{aligned} &\sqrt{\Delta_0^2 + (|\mu - 2t\overline{\alpha}_b \cos q_y| + |2t\overline{\alpha}_a \cos q_{x1}|)^2} > B \\ &> \sqrt{\Delta_0^2 + (|\mu - 2t\overline{\alpha}_b \cos q_y| - |2t\overline{\alpha}_a \cos q_{x1}|)^2}, \end{aligned} \tag{8}$$

where $\overline{\alpha}_\delta = (\alpha_\delta + \alpha^*_\delta)/2 = \cos(\mathbf{Q}\cdot\boldsymbol{\delta}/2)$. We observe that setting $\overline{\alpha}_b = 0$ and $q_{x1} = 0$ recovers the well-known 1D result of Ref. [15].

Equation (8) is the general criterion for the appearance of Majorana states at momentum q_y and represents one of the central results of this paper. It applies to any noncollinear magnet with spiral, helical, or tilted conical order, of arbitrary wavelength and direction, in proximity to an s-wave superconductor. Criterion (8) can be extended in a straightforward manner to include longer-range hopping in the first term of Eq. (1). From the unitary transformation that leads to Eq. (5), one sees that longer-range hopping induces higher harmonic p-wave pairing. For simplicity, in the following we focus on nearest-neighbor hopping, which is likely the dominant term in any experimentally relevant system.

Condition (8) for the existence of Majorana states is corroborated by our numerical simulations. Using the spin-generalized Bogoliubov transformation $g_{i\sigma} = \sum_{n,\alpha} (u_{\text{in}\sigma\alpha}\gamma_{n\alpha} + v^*_{\text{in}\sigma\alpha}\gamma^\dagger_{n\alpha})$, we numerically diagonalize Hamiltonian (4) with the aforementioned boundary conditions. Figure 1(b) shows a typical dispersion $E(n, q_y)$, which displays Majorana zero-energy states in the q_y's that satisfy Eq. (8). Note that since Eq. (8) can be satisfied even when $\mu = 0$, the chemical potential in general does not need to be adjusted. Consequently, the edge states can occur in an isolated sample without attaching any leads. The $2t\overline{\alpha}_b \cos q_y$ factor in Eq. (8) greatly enlarges the number of q_y's that can satisfy the Majorana condition. Hence, it increases the chance to observe Majorana fermions, as one can see from the phase diagram for a planar spiral propagating along $\mathbf{Q} \propto (1,0)$; see Fig. 1(a). We note that the phase diagram of the 2D model (1) has a much larger topologically nontrivial phase in the $B_0 - \overline{\alpha}$ space [38] than the 1D model [15].

The localized Majorana edge states reveal themselves as zero-bias peaks (ZBPs) in the local density of states (LDOS)

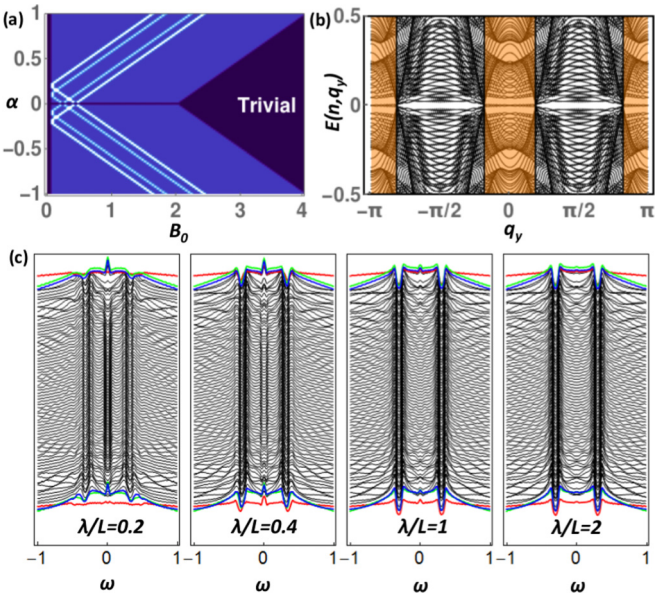

FIG. 1. (Color online) (a) Topological phase diagram of the 2D model, given by Eq. (1), as a function of $s-d$ coupling B_0 and pitch angle $\alpha \equiv \overline{\alpha}_a = \cos(\mathbf{Q}\cdot\mathbf{a}/2)$ for an in-plane spiral (i.e., $B_\perp = 0$) propagating along $\mathbf{Q} \propto (1,0)$ and at $\mu = 0$. The topologically nontrivial phase corresponds to the blue region. For comparison, the nontrivial phase of the 1D model with $\mu = -0.2$ and -0.4 is shown as the region inside the light blue and white dots, respectively. Other noncollinear orders, such as helical and tilted conical orders propagating along various directions, exhibit similar phase diagrams. (b) Energy levels of a system with size $L = 80a$ subject to an in-plane spiral of wave length $\lambda = 2\pi/|\mathbf{Q}| = 16a$ with $B_0 = 0.3$ and $\mathbf{Q} \propto (1,0)$. The orange regions are the q_y's at which the topological criterion given by Eq. (8) is satisfied, where one also sees the Majorana zero-energy edge states. (c) LDOS along $\hat{\mathbf{x}}$ for different values of λ/L. Red, green, and blue lines are the first, second, and third sites away from the edge, respectively. The $\lambda/L = 2$ case corresponds to a Neel or Bloch domain wall in a ferromagnetic insulator. Other parameters are $t = -1$ and $\Delta = 0.05$.

at the edge of the sample [Fig. 1(c)]. Three gaplike features show up in the LDOS. The feature near zero energy represents the induced $(p_x + p_y)$-wave gap in Eq. (5). The two gaplike structures at larger energy $\omega \neq 0$ come from the bulk gap Δ shifted by $\pm B_0$, which typically has a magnitude of $\sim$0.01–1 eV [39], so $B_0 > \Delta$ is anticipated. The weight of the ZBP decreases as the spiral wavelength $\lambda = 2\pi/|\mathbf{Q}|$ increases. The $\lambda/L = 2$ case corresponds to a Neel or Bloch magnetic domain wall joining two regions of opposite spin orientations in a ferromagnetic insulator, since it can be viewed as a spiral with half a wavelength, and the interface to an SC can be described by Eqs. (1)–(8). In such case, the ZBP is small but still discernible. We remark that a single domain of multiferroics can reach millimeter size [40], which may help to separate the Majorana pairs over macroscopic distances.

We have checked that even if the multiferroic contains domains of different spiral chirality, or the spins have small deviations from the perfectly periodic texture, the Majorana states still exist at the edge of the sample or at boundaries between domains. Moreover, edge roughness and edge disorder are expected to have only small effects on the Majorana states [41–43], as they arise as a consequence of the quantized bulk invariant (7). That is, translation symmetry along the edge is not crucial for the protection of the Majorana states.

III. SC/SKYRMION INTERFACE

Skyrmion spin textures have been observed in thin-film insulating multiferroics [44,45] at temperatures approaching the typical SC transition temperature, in the presence of a small magnetic field that presumably has negligible effect on the SC. To gain more understanding about the SC/skyrmion insulator interface, disregarding external magnetic fields, we first consider a closely related pedagogical model defined on a square lattice ribbon, whose low-energy sector can be studied analytically. The spin texture of this model is shown in Fig. 2(a). It induces a magnetic field $\mathbf{B}_i$ at the interface with the SC, where $\mathbf{B}_i$ at the position (r_i,φ_i) of the square lattice is given by

$$\mathbf{B}_i = B(\sin\theta_i\cos\varphi_i, \sin\theta_i\sin\varphi_i, \cos\theta_i), \tag{9}$$

with $\theta_i = \pi r_i/R$, and R is the width of the ribbon in the $\hat{\mathbf{r}}$ direction. We assume OBC along the $\hat{\mathbf{r}}$ direction and PBC along the $\hat{\boldsymbol{\varphi}}$ direction. The Hamiltonian is described by Eq. (1) with $\hat{\boldsymbol{\delta}} = \{\hat{\mathbf{r}},\hat{\boldsymbol{\varphi}}\}$. To align the spin texture along σ^z, one performs the rotation in Eq. (3) with U_i defined by

$$U_i = \begin{pmatrix} \cos\frac{\theta_i}{2} & -\sin\frac{\theta_i}{2}e^{-i\varphi_i} \\ \sin\frac{\theta_i}{2}e^{i\varphi_i} & \cos\frac{\theta_i}{2} \end{pmatrix}, \tag{10}$$

which yields Eq. (4) with

$$\begin{aligned} \alpha_{i\varphi} &= 1 + 2ie^{i\pi/N_\varphi}\sin^2\left(\frac{\theta_i}{2}\right)\sin\frac{\pi}{N_\varphi}, \quad \alpha_{ir} = \cos\frac{\pi}{N_r}, \\ \beta_{i\varphi} &= i\sin\theta_i e^{i(\varphi_i+\varphi_{i+\varphi})/2}\sin\frac{\pi}{N_\varphi} \equiv e^{i(\varphi_i+\varphi_{i+\varphi})/2}\tilde{\beta}_{i\varphi}, \\ \beta_{ir} &= e^{i\varphi_i}\sin\frac{\pi}{N_r} \equiv e^{i\varphi_i}\tilde{\beta}_{ir}, \end{aligned} \tag{11}$$

where N_r and N_φ are the number of sites in each direction. After gauging away the extra phase $\beta_{i\delta} \to \tilde{\beta}_{i\delta}$ by $e^{-i\varphi_i/2}g_{i\downarrow} \to g_{i\downarrow}$ and $e^{i\varphi_i/2}g_{i\uparrow} \to g_{i\uparrow}$, the Hamiltonian is translationally invariant along $\hat{\boldsymbol{\varphi}}$ but not along $\hat{\mathbf{r}}$ because $\tilde{\beta}_{i\varphi} \propto \sin\theta_i = \sin(\pi r_i/R)$. In the $B \approx |\mu| \gg \{t_\delta,\Delta_0\}$ limit, using Eq. (5) of the low-energy effective theory, the induced gap along $\hat{\mathbf{r}}$ and $\hat{\boldsymbol{\varphi}}$ is proportional to $\tilde{\beta}^*_{ir}$ and $\tilde{\beta}^*_{i\varphi}$, and therefore of $(p_r + ip_\varphi)$-wave-like symmetry.

The spin-conserving $\alpha_{i\delta}t_{i\delta}$ and spin-flipping $\beta_{i\delta}t_{i\delta}$ hopping in the $g_{i\sigma}$ basis contain an emergent electromagnetic (EM) field [46,47] coming from the spatial dependence of the unitary transformation (10) [48]. This becomes evident in the continuous limit $\theta_i \to \theta$, $\varphi_i \to \varphi$, $U_i \to U$, and using $\int_0^{a_r} dr\,\partial_r\theta = 2\pi/N_r \ll 1$ and $\int_0^{a_\varphi} d\varphi\,\partial_\varphi\varphi = 2\pi/N_\varphi \ll 1$. The α_δ and β_δ contain the phase gained over one lattice constant,

$$\Omega_\delta = \begin{pmatrix} \alpha_\delta & -\beta^*_\delta \\ \beta_\delta & \alpha^*_\delta \end{pmatrix} = e^{-iq\int_0^{a_\delta} d\delta A_\delta}, \tag{12}$$

where $A_\delta = i(\hbar/q)U^\dagger\partial_\delta U$. The factor of i difference between A_r and A_φ eventually leads to the induced $(p_r + ip_\varphi)$-wave-like gap. Figure 2(d) shows the dispersion of this pedagogical model. For comparison, we show in Fig. 2(e) the dispersion when the emergent EM field is manually turned off by setting

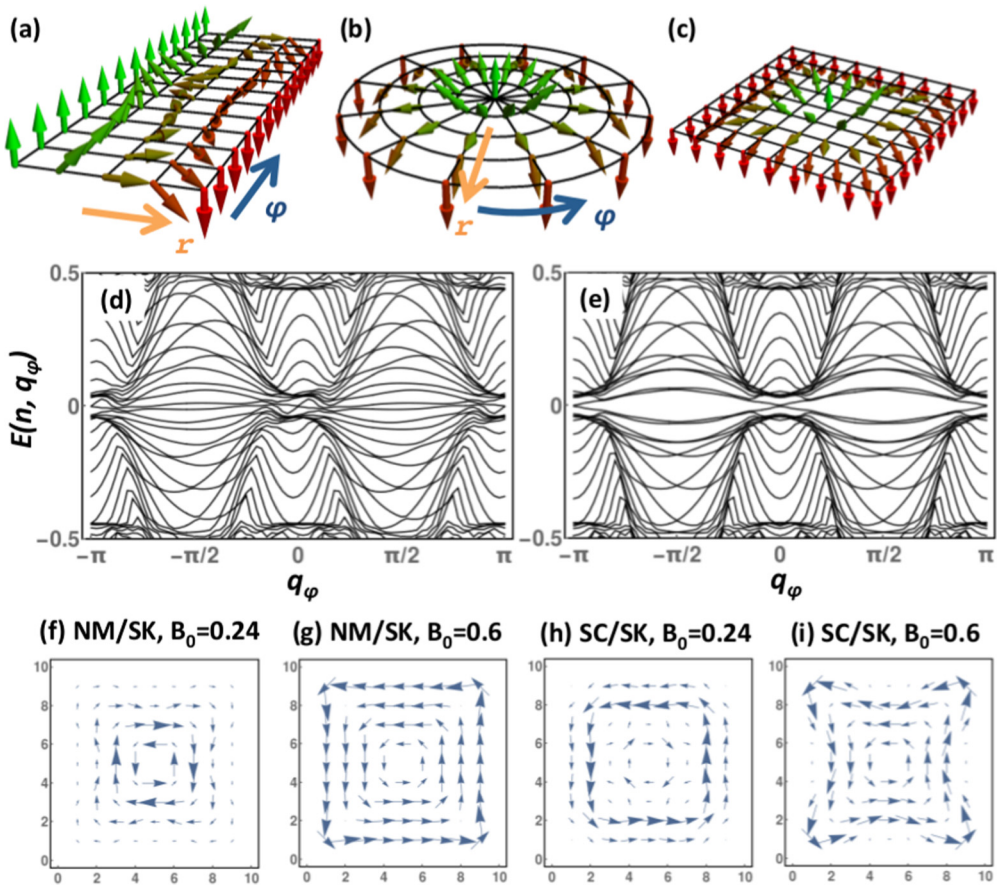

FIG. 2. (Color online) (a) Spin texture of the pedagogical model, which is closely related to the spin texture of a single nonchiral skyrmion on (b) a polar lattice and (c) a square lattice. (d),(e) Energy bands of the pedagogical model with OBC in $\hat{\mathbf{r}}$ and PBC in $\hat{\boldsymbol{\varphi}}$, with $N_r = N_\varphi = 40$ and $B_0 = 0.24$, in (d) the presence and (e) the absence of the emergent EM field. (f)–(i) Spontaneous current patterns at the interface between an s-wave SC and a single nonchiral skyrmion on a square lattice with size 9×9 for (f),(g) the normal state ($\Delta = 0$) and (h),(i) the superconducting state ($\Delta = 0.2$). Parameters are $t = -1$ and $\mu = -0.1$.

$\alpha_{i\varphi} = 1$ in Eq. (11). Without the emergent EM field, the dispersive edge bands expected for the induced $(p_r + ip_\varphi)$-wave-like gap are evident, whereas in the presence of it the bulk gap is diminished, although the trace of edge bands can still be seen in some cases [compare $q_\varphi \approx 0$ and $E(n,q_\varphi) \approx 0$ regions in Figs. 2(d) and 2(e)].

The relevance of this pedagogical model is made clear by shrinking the spins at the $r_i = 0$ edge [green arrows in Fig. 2(a)] into one single spin, which results in a nonchiral skyrmion on a polar lattice shown in Fig. 2(b), with the same interface magnetic field described by Eq. (9). Certainly these two lattices cannot be mapped to each other exactly, but their low-energy sectors display similar features.

The pedagogical model indicates that the SC/skyrmion interface hosts a complex interplay between (i) the s-wave gap, (ii) the induced $(p_r + ip_\varphi)$-wave-like gap, (iii) the emergent EM field, and (iv) the $s - d$ coupling B_0. Motivated by the recent observation of a single skyrmion generated by a scanning tunneling microscope tip [49] (although with an external magnetic field), we proceed to study the SC/skyrmion interface on an open square. The skyrmion spin texture $\mathbf{B}_i$ on a square is shown in Fig. 2(c) and is described by Eq. (9) with $\theta_i = \pi|\mathbf{r}_i|/R(\mathbf{r}_i)$, where $R(\mathbf{r}_i)$ is the length of the straight line that connects the center of the square with the edge while passing through the point $\mathbf{r}_i = (x_i, y_i) = |\mathbf{r}_i|(\cos\varphi_i, \sin\varphi_i)$. The spontaneous current at site i can be calculated from Eq. (1) by

$$\mathbf{J}_i = -i \sum_{\sigma,\delta} t_\delta \boldsymbol{\delta} \langle f^\dagger_{i+\delta\sigma} f_{i\sigma} \rangle. \tag{13}$$

As shown in Figs. 2(f) and 2(g), even in the normal state, i.e., at the normal-metal/skyrmion interface, there is a persistent current whose vorticity strongly depends on the emergent EM field, the $s - d$ coupling B_0, and the value of μ. In the superconducting state, the $(p_r + ip_\varphi)$-wave-like pairing gives rise to an additional topological edge current which is added to the persistent current; see Figs. 2(h) and 2(i). For $B_0 \gg \Delta$, the current pattern in the SC state recovers that of the normal state, as can be seen by comparing Figs. 2(g) and 2(i). Our results suggest that in an SC/skyrmion *lattice* interface, the current pattern will exhibit a vortexlike structure.

IV. CONCLUSION

In summary, we have shown that topological superconductivity can be proximity induced at an interface between an s-wave SC and an insulating multiferroic or a magnetic domain wall. We have presented a general criterion for the

appearance of Majorana edge states at these interfaces, which is applicable to multiferroic insulators with helical, cycloidal, and tilted conical order, as well as Bloch and Neel magnetic domain walls of collinear magnetic insulators. Our results show that Majorana flat bands appear in these heterostructures for a large region of parameter space and that, in general, fine tuning of the chemical potential is not necessary. Furthermore, a skyrmion spin texture in proximity to an s-wave SC is shown to induce a $(p_r + ip_\varphi)$-wave-like pairing. This topologically nontrivial interface SC supports both bulk persistent currents, which arise due to an emergent EM field, and topological edge currents. We anticipate that our findings facilitate the experimental realization of topological superconductivity in artificial heterostructures and the detection of its Majorana states.

ACKNOWLEDGMENT

We thank P. W. Brouwer, Y.-H. Liu, and F. von Oppen for stimulating discussions.

[1] C. Nayak, S. H. Simon, A. Stern, M. Freedman, and S. Das Sarma, Rev. Mod. Phys. **80**, 1083 (2008).
[2] J. Alicea, Rep. Prog. Phys. **75**, 076501 (2012).
[3] C. Beenakker, Ann. Rev. Condens. Matter Phys. **4**, 113 (2013).
[4] S. R. Elliott and M. Franz, Rev. Mod. Phys. **87**, 137 (2015).
[5] T. D. Stanescu and S. Tewari, J. Phys. Condens. Matter **25**, 233201 (2013).
[6] A. P. Schnyder and P. M. R. Brydon, J. Phys.: Condens. Matter **27**, 243201 (2015).
[7] A. Kitaev, Phys. Usp. **44**, 131 (2001).
[8] Y. Oreg, G. Refael, and F. von Oppen, Phys. Rev. Lett. **105**, 177002 (2010).
[9] R. M. Lutchyn, J. D. Sau, and S. Das Sarma, Phys. Rev. Lett. **105**, 077001 (2010).
[10] J. D. Sau, R. M. Lutchyn, S. Tewari, and S. Das Sarma, Phys. Rev. Lett. **104**, 040502 (2010).
[11] V. Mourik, K. Zuo, S. M. Frolov, S. R. Plissard, E. P. A. M. Bakkers, and L. P. Kouwenhoven, Science **336**, 1003 (2012).
[12] A. Das, Y. Ronen, Y. Most, Y. Oreg, M. Heiblum, and H. Shtrikman, Nat. Phys. **8**, 887 (2012).
[13] K. Sun and N. Shah, Phys. Rev. B **91**, 144508 (2015).
[14] T.-P. Choy, J. M. Edge, A. R. Akhmerov, and C. W. J. Beenakker, Phys. Rev. B **84**, 195442 (2011).
[15] S. Nadj-Perge, I. K. Drozdov, B. A. Bernevig, and A. Yazdani, Phys. Rev. B **88**, 020407 (2013).
[16] B. Braunecker and P. Simon, Phys. Rev. Lett. **111**, 147202 (2013).
[17] F. Pientka, L. I. Glazman, and F. von Oppen, Phys. Rev. B **88**, 155420 (2013).
[18] J. Klinovaja, P. Stano, A. Yazdani, and D. Loss, Phys. Rev. Lett. **111**, 186805 (2013).
[19] M. M. Vazifeh and M. Franz, Phys. Rev. Lett. **111**, 206802 (2013).
[20] F. Pientka, L. I. Glazman, and F. von Oppen, Phys. Rev. B **89**, 180505 (2014).
[21] J. Röntynen and T. Ojanen, Phys. Rev. B **90**, 180503 (2014).
[22] Y. Kim, M. Cheng, B. Bauer, R. M. Lutchyn, and S. Das Sarma, Phys. Rev. B **90**, 060401 (2014).
[23] P. M. R. Brydon, S. Das Sarma, H.-Y. Hui, and J. D. Sau, Phys. Rev. B **91**, 064505 (2015).
[24] K. Pöyhönen, A. Westström, J. Röntynen, and T. Ojanen, Phys. Rev. B **89**, 115109 (2014).
[25] L. Yu, Acta Phys. Sin. **21**, 75 (1965).
[26] H. Shiba, Prog. Theor. Phys. **40**, 435 (1968).
[27] A. I. Rusinov, Zh. Eksp. Teor. Fiz. Pisma Red. **9**, 146 (1968).
[28] S. Nadj-Perge, I. K. Drozdov, J. Li, H. Chen, S. Jeon, J. Seo, A. H. MacDonald, B. A. Bernevig, and A. Yazdani, Science **346**, 602 (2014).
[29] J. D. Sau and P. M. R. Brydon, Phys. Rev. Lett. **115**, 127003 (2015).
[30] S. Nakosai, Y. Tanaka, and N. Nagaosa, Phys. Rev. B **88**, 180503 (2013).
[31] G. Deutscher and F. Meunier, Phys. Rev. Lett. **22**, 395 (1969).
[32] J. J. Hauser, Phys. Rev. Lett. **23**, 374 (1969).
[33] P. D. Gennes, Phys. Lett. **23**, 10 (1966).
[34] Y. Yamasaki, H. Sagayama, T. Goto, M. Matsuura, K. Hirota, T. Arima, and Y. Tokura, Phys. Rev. Lett. **98**, 147204 (2007).
[35] Y. Yamasaki, H. Sagayama, N. Abe, T. Arima, K. Sasai, M. Matsuura, K. Hirota, D. Okuyama, Y. Noda, and Y. Tokura, Phys. Rev. Lett. **101**, 097204 (2008).
[36] T. Kimura and Y. Tokura, J. Phys. Condens. Matter **20**, 434204 (2008).
[37] H. Murakawa, Y. Onose, F. Kagawa, S. Ishiwata, Y. Kaneko, and Y. Tokura, Phys. Rev. Lett. **101**, 197207 (2008).
[38] The (weak) topological phase [42] in 2D is judged by whether any q_y satisfies Eq. (8) at a given $(B_0,\overline{\alpha})$.
[39] Y. Kajiwara, K. Harii, S. Takahashi, J. Ohe, K. Uchida, M. Mizuguchi, H. Umezawa, H. Kawai, K. Ando, K. Takanashi *et al.*, Nature (London) **464**, 262 (2010).
[40] R. D. Johnson, P. Barone, A. Bombardi, R. J. Bean, S. Picozzi, P. G. Radaelli, Y. S. Oh, S.-W. Cheong, and L. C. Chapon, Phys. Rev. Lett. **110**, 217206 (2013).
[41] R. Queiroz and A. P. Schnyder, Phys. Rev. B **89**, 054501 (2014).
[42] N. Sedlmayr, J. M. Aguiar-Hualde, and C. Bena, Phys. Rev. B **91**, 115415 (2015).
[43] C. L. M. Wong, J. Liu, K. T. Law, and P. A. Lee, Phys. Rev. B **88**, 060504 (2013).
[44] S. Seki, X. Z. Yu, S. Ishiwata, and Y. Tokura, Science **336**, 198 (2012).
[45] S. Seki, S. Ishiwata, and Y. Tokura, Phys. Rev. B **86**, 060403 (2012).
[46] T. Schulz, R. Ritz, A. Bauer, M. Halder, M. Wagner, C. Franz, C. Pfleiderer, K. Everschor, M. Garst, and A. Rosch, Nat. Phys. **8**, 301 (2012).
[47] N. Nagaosa and Y. Tokura, Nat. Nanotechnol. **8**, 899 (2013).
[48] S. Zhang and Steven S.-L. Zhang, Phys. Rev. Lett. **102**, 086601 (2009).
[49] N. Romming, C. Hanneken, M. Menzel, J. E. Bickel, B. Wolter, K. von Bergmann, A. Kubetzka, and R. Wiesendanger, Science **341**, 636 (2013).